Superconductivity in the Mn_5Si_3-type Zr_5Sb_3 system

B. Lv,[1,*] X. Y. Zhu,[1] B. Lorenz,[1] F. Y. Wei,[1] Y. Y. Xue,[1] Z. P. Yin,[2] G. Kotliar,[2] and C. W. Chu[1,3,*]

[1]*Department of Physics and Texas Center for Superconductivity, University of Houston, Houston, Texas 77204-5002, USA*

[2]*Department of Physics and Astronomy, Rutgers University, Piscataway, New Jersey 08854-8019, USA*

[3]*Lawrence Berkeley National Laboratory, Berkeley, California 94720, USA*

(Received 24 September 2013; revised manuscript received 10 October 2013; published 28 October 2013)

We report the discovery of superconductivity at 2.3 K in Zr_5Sb_3, the first superconducting member in the large compound family of the Mn_5Si_3-type structure. Transport, magnetic, and calorimetric measurements clearly demonstrate bulk superconductivity for Zr_5Sb_3 and suggest it to be a possible phonon-mediated BCS superconductor with a relatively large density of states at the Fermi level associated with the *d* electrons of Zr and substantially larger electron-phonon coupling compared to the Sn counterpart compound Zr_5Sn_3 from band structure calculations. More superconductors with even higher transition temperatures are expected to be found in this family of compounds.

DOI: 10.1103/PhysRevB.88.134520 PACS number(s): 74.90.+n, 74.70.Ad, 74.20.Pq, 71.38.−k

Searching for superconductivity in materials of new, distinct structural classes has been a major endeavor since the discovery of the phenomenon. Discovering superconductors in various material families has proven to be fruitful in achieving superconductivity with higher transition temperature T_c or realizing novel mechanisms. For instance, it was the unexpected observation of superconductivity in 1979 in $CeCu_2Si_2$ that heralded in the exciting systems of heavy fermions, despite its initial low $T_c \sim 1$ K.[1] It was the discovery of superconductivity in the omnipresent perovskite-like-layered cuprates, first at 35 K in Ba-doped La_2CuO_4 in 1986[2] and then at 93 K in $YBa_2Cu_3O_7$ in 1987,[3] that inaugurated the modern era of high-temperature superconductivity for exciting science and technology in the ensuing decades till today. Then, it was the detection of superconductivity in 2008 in layered Fe-based compounds, F-doped LaFeAsO with an unusually high $T_c \sim 26$ K,[4] that has opened up a new opportunity in unraveling the high-temperature superconducting mechanism and has offered new hopes for superconductors of high T_c due to the presence of a large amount of magnetic Fe element. We have, therefore, decided to explore compounds of a structural class that consists of large number of compounds where superconductivity is likely but has not yet been found.

We have chosen to investigate the binary A_5B_3 system where A = early transition metal or rare earth elements and B = IIIB–VB elements. The compound family A_5B_3 has been shown to consist of more than 590 compounds with three distinct structure-types, i.e., hexagonal Mn_5Si_3 type ($P6_3/mcm$) with ∼440 compounds, tetragonal Cr_5B_3 type ($I4/mcm$) with ∼86 compounds, and Yb_5Sb_3 type ($Pnma$) with ∼65 compounds.[5] There exists no report of superconductivity in the large compound family of Mn_5Si_3 type to date. In view of the possible large electron density of states (DOS) associated with the *d* electrons in the transition metal elements that may give rise to superconductivity, we have carried out detailed structural, magnetic, transport, and calorimetric studies of the hexagonal Mn_5Si_3 structure type Zr_5X_3 compounds for X = Sb, Sn, Ge, Ga, and Al. Superconductivity at ∼2.3 K has been discovered in Zr_5Sb_3, although not in the other members tested, possibly due to their much smaller electron DOS and weaker electron-phonon coupling. Zr_5Sb_3, therefore, represents the first superconducting member of this large compound family of Mn_5Si_3 type and gives hope that many others even with higher T_c may be found.

Samples were prepared through arc-melting pellets of Zr and X in a nominal composition of 5:3 + δ on a water-cooled copper hearth in a homemade arc furnace in argon-atmosphere with a Zr gas getter. For the volatile element X, such as Sb, δ is greater than 0, e.g., $\delta \sim 0.3$, to compensate for the loss of Sb through vaporization when the pellet is first brought close to the arc. The X elements are pieces from Sigma Aldrich with >99.999% purity and are used as received. The Zr is purchased from Alfa Aesar and further purified through decomposition of ZrH_2 as described previously.[6,7]

X-ray powder diffraction was performed using a Panalytical X'pert diffractometer. The dc magnetic susceptibility $\chi(T)$ and $\chi(H)$ was measured using a Quantum Design Magnetic Property Measurement System (MPMS) down to 2 K and up to 5 T. Electrical resistivity $\rho(T)$ and $\rho(H)$ was measured by employing a standard four-probe method using a Linear Research LR-400 ac bridge operated at 15.9 Hz in a Quantum Design Physical Property Measurement System (PPMS) up to 7 T and down to 1.9 K. The specific heat $C_p(T)$ measurement was determined down to 0.4 K in a field up to 7 T using the Quantum Design He3-attachment in the Quantum Design PPMS.

The hexagonal Mn_5Si_3-type compounds have been widely studied previously in terms of their structure, stoichiometry, and host-interstitial chemistry, particularly for the Zr-based compounds.[6–9] In the hexagonal Zr_5X_3 (X = Sb, Ga, Ge, and Sn) compounds, there are three distinct crystallographic sites. As shown in Fig. 1, the trigonal antiprisms consisting of Zr1 atoms are face shared and form a column along the *c* axis. The shared faces are then each bridged by three X atoms to give $Zr_{6/2}X_{6/2}$ chains. Each of the Zr1 atoms has six Zr and four X neighbor atoms. Meanwhile, a parallel linear chain comprised of Zr2 atoms is closely bonded with the $Zr_{6/2}X_{6/2}$ chain. The Zr2 atoms are neighbored with six X forming a twisted trigonal prism. The octahedral interstitial sites formed by the Zr1 trigonal antiprism atoms are ideal for small atoms to occupy. In fact, a variety of compounds Zr_5Sb_3Z have been discovered, with interstitial guest atoms Z = C, O, Al, Si, P, S, Co, Ni, Cu, Zn, Ge, As, Se, Ru, and Ag occupying the centers

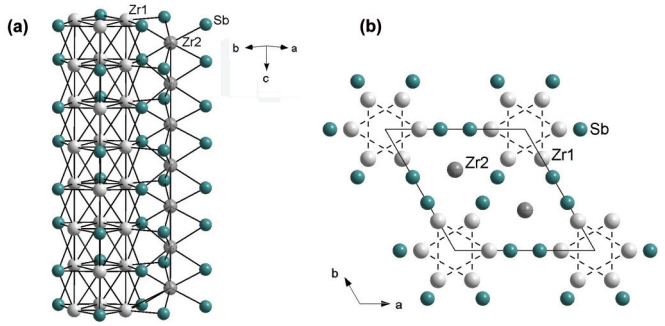

FIG. 1. (Color online) Crystal structure of Zr_5Sb_3: (a) side view; (b) [001] projection. Two types of Zr atoms are labeled differently for distinction.

of zirconium trigonal antiprismatic sites in the Zr_5Sb_3 host.[8] Band structural calculations have shown that the zirconium states and electrons are diverted from the broad conduction band to form the Zr-Z bonds.[8]

Polycrystalline samples of Zr_5X_3 (X = Sb, Al, Ga, Ge, and Sn) were synthesized through the arc-melting method. Figures 2(a) and 2(b) show the x-ray Rietveld refinement patterns of Zr_5Sb_3 and Zr_5Sn_3, respectively. The sharp peaks and good refinement values of Rp and Rwp (Rp = 4.60%, Rwp = 7.11% for Zr_5Sb_3 and Rp = 5.38%, Rwp = 7.58% for Zr_5Sn_3) demonstrate that they possess the hexagonal Mn_5Si_3 structure type. The refined lattice parameters are a = 8.4053(3) Å and c = 5.7640(3) Å for Zr_5Sb_3, a = 8.4606(3) Å and c = 5.7771(2) Å for Zr_5Sn_3, and match well with previous studies.[7,10] A few minor peaks are also found in the x-ray powder patterns of Zr_5Sb_3 [marked by red stars in Fig. 2(a)], estimated to be less than 5% of the major peaks intensity and possibly due to the orthorhombic Y_5Bi_3-type Zr_5Sb_3. The metallic gray ingots after arc melting are moderately stable for a few hours in humid air before turning into black powder.

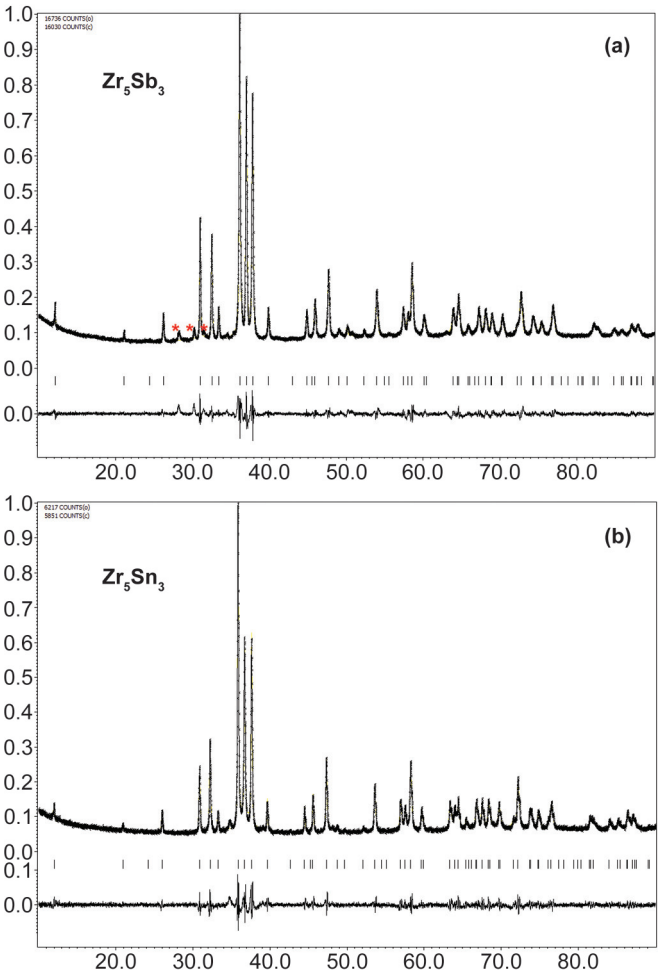

FIG. 2. (Color online) Rietveld refinement of (a) Zr_5Sb_3 (impurity peaks marked by red stars) and (b) Zr_5Sn_3 x-ray powder pattern.

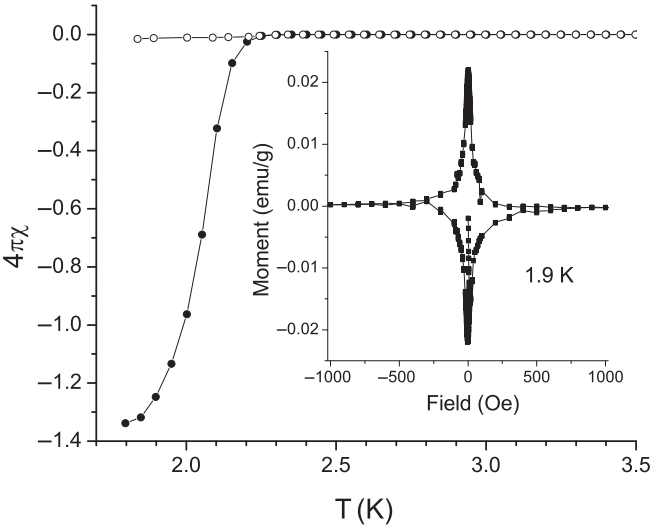

FIG. 3. ZFC susceptibility (solid circles) and FC susceptibility (open circles) data at 5 Oe for Zr_5Sb_3 sample. Inset: M-H curve at 1.9 K.

The superconductivity in Zr_5Sb_3 is evident from the magnetic susceptibility $\chi(T)$, electrical resistivity $\rho(T,H)$, and the specific-heat $C_p(T)$ measurements. Figure 3 displays the $\chi(T)$ measured at 5 Oe both in the zero-field-cooled (ZFC) and field-cooled (FC) modes. A clear diamagnetic shift is observed below 2.3 K. The shielding volume fraction from ZFC-$\chi(T)$ is ~1.3 before demagnetization correction, in conjunction with the FC-$\chi(T)$, indicating bulk superconductivity for the sample. The $M(H)$ curve at 1.9 K in the inset shows clear type-II superconductor characteristics, with a low critical field $H_{c1} < 5$ Oe.

The electrical resistivity $\rho(T)$ of Zr_5Sb_3 is shown in Fig. 4, with a room-temperature value of 0.36 mΩ cm. It decreases with decreasing temperature, typical for a metal, and drops sharply below 2.3 K, characteristic of a superconducting transition. The transition width is estimated to be 0.2 K from 10 to 90% resistivity drops. In the presence of magnetic fields, the superconducting transition is systematically shifted to lower temperature and suppressed to below 1.9 K at 7 kOe, as shown in the inset of Fig. 4.

The bulk superconductivity of the compound is further demonstrated by the pronounced specific-heat C_p anomaly, as shown in Fig. 5. The superconducting transition is suppressed to below 0.4 K in a magnetic field of 30 kOe (Fig. 5). The electronic Sommerfeld coefficient γ and Debye temperature θ_D are 24.1 mJ/(mol K^2) and ~240 K, respectively. The electronic contribution to the heat capacity C_{el} in the

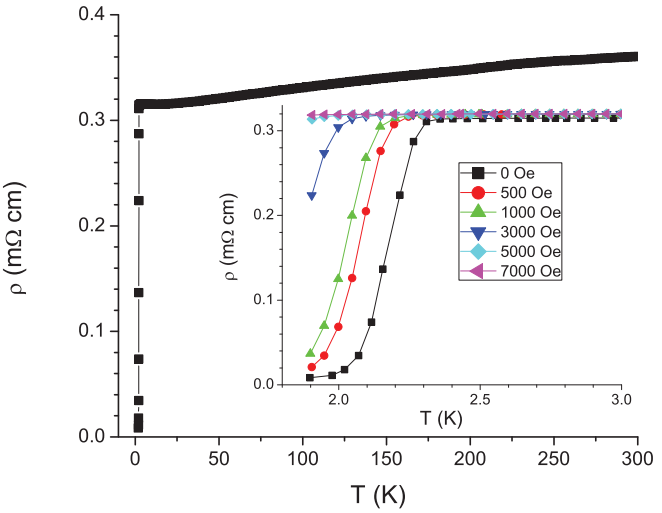

FIG. 4. (Color online) Resistivity data of Zr_5Sb_3 at $H = 0$ between 1.9 and 300 K. Inset: resistivity data under different magnetic fields between 1.9 and 3.0 K.

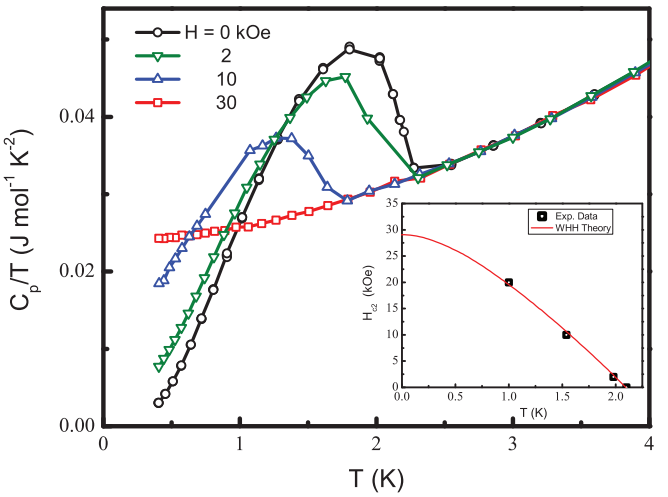

FIG. 6. (Color online) Field dependence of the heat capacity of Zr_5Sb_3. The inset shows the upper critical field vs temperature (open squares) and the fit to the WHH theory (red line).

superconducting state is determined by subtracting the 30-kOe data. The normalized $C_{el}/(\gamma\ T)$ as a function of the reduced temperature, T/T_c, is plotted in the inset of Fig. 5 and compared with the theory. The BCS theory (dashed line) does not fit the data well; however, the modification of the superconducting gap, as described by the α-model,[11] leads to a good description of the experimental data. In magnetic fields, the heat capacity peak is shifted to lower temperature, as expected for the superconducting state. Data in different external fields are shown in Fig. 6. The upper critical field $H_{c2}(T)$ is derived from the heat capacity data and shown in the inset of Fig. 6. The extrapolation of H_{c2} to zero temperature is done by fitting the data to the Werthamer-Helfand-Hohenberg (WHH) theory,[12] shown as the red line in the figure. $H_{c2}(0)$ is indeed found to be less than 30 kOe, as already suggested by the heat capacity data of Fig. 6. Unfortunately, the isostructural Zr_5Sn_3 was found not to be superconducting. Its C_p reveals a much smaller Sommerfeld coefficient = 14 mJ/(mol K^2) and Debye temperature $\theta_D = \sim$280 K. Since γ in normal metals is proportional to the electronic DOS at the Fermi level E_F, a 40% lower value may explain the missing superconducting state in Zr_5Sn_3.

The band structures and the DOS at the Fermi level of both Zr_5Sb_3 and Zr_5Sn_3 have been calculated. Zr_5Sb_3 has bands at the Fermi level that are much more strongly coupled to phonons than in Zr_5Sn_3, indicating Zr_5Sb_3 has a much stronger electron-phonon coupling than Zr_5Sn_3.[13] The DOS of Zr_5Sb_3 at the Fermi level is about 2.4 times higher than that of Zr_5Sn_3, as shown in Fig. 7, in good agreement with the results of the C_p experiments. Therefore, the observed superconductivity in Zr_5Sb_3 is possibly of the BCS type arising from decent electron-phonon interaction as well as its high DOS at the F_F due to the d electrons of Zr.

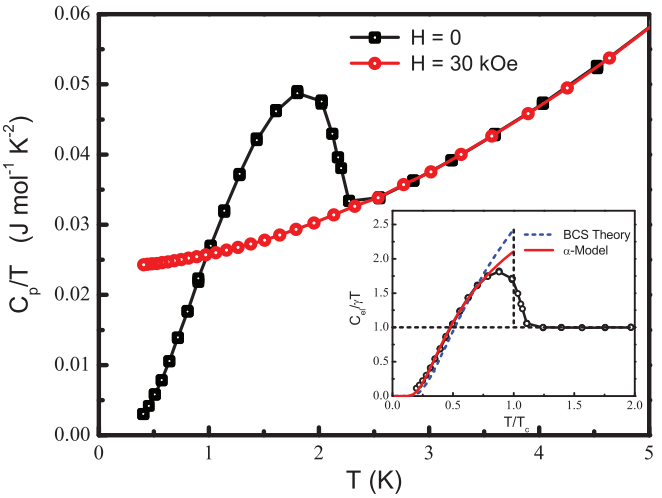

FIG. 5. (Color online) Heat capacity of Zr_5Sb_3 at zero field (open squares) and at $H = 30$ kOe (open red circles). The inset shows the normalized electronic heat capacity in comparison with the BCS and α-models ($\alpha = 1.55$).

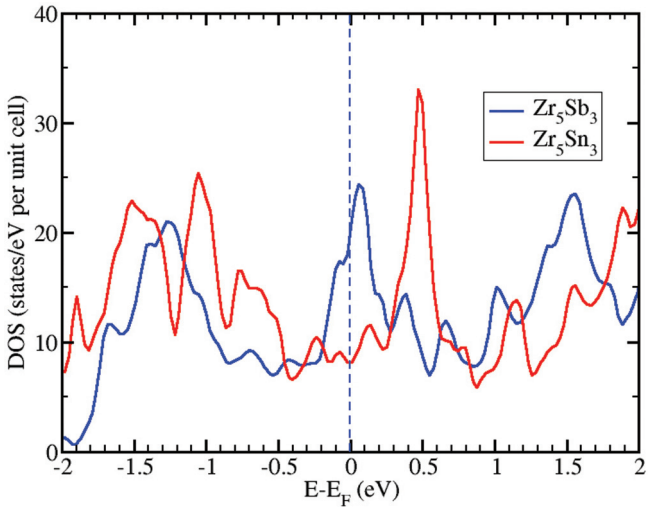

FIG. 7. (Color online) The DOS of Zr_5Sb_3 and Zr_5Sn_3 calculated by density functional theory with the generalized gradient approximation exchange-correlation functional (Ref. 14).

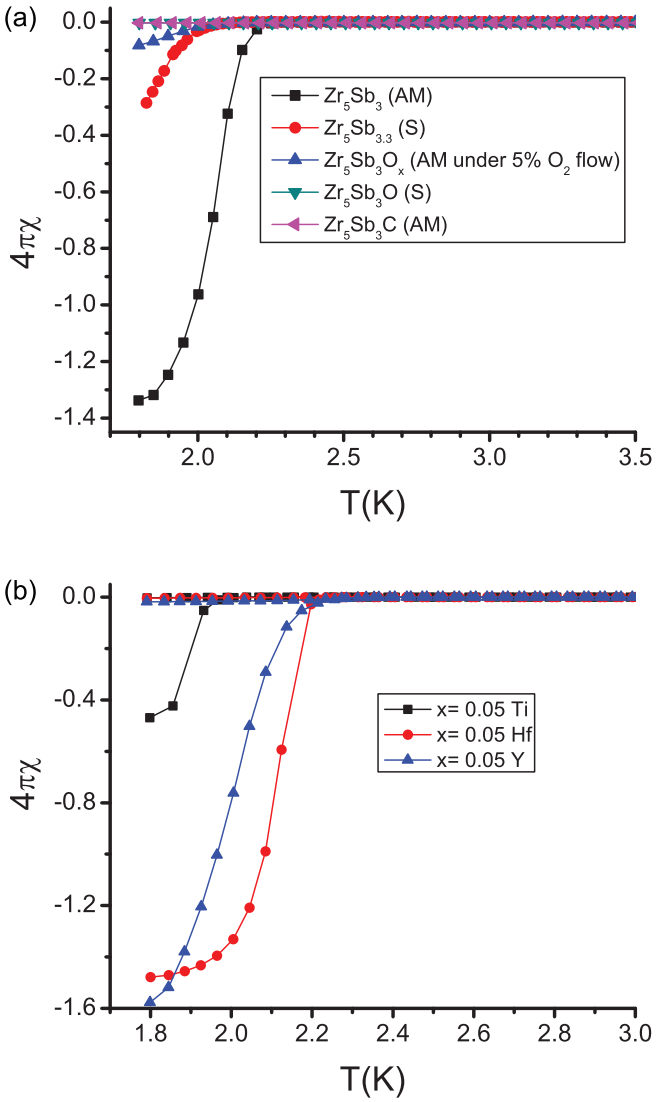

FIG. 8. (Color online) (a) ZFC susceptibilities under 5-Oe field for Zr_5Sb_3, $Zr_5Sb_{3.3}$, $Zr_5Sb_3O_x$, Zr_5Sb_3O, and Zr_5Sb_3C. Abbreviations: AM = arc melted; S = sintered. (b) ZFC and FC susceptibilities under 5-Oe field for different $(Zr_{1-x}M_x)_5Sb_3$ (M = Ti, Hf, and Y) samples.

Both hexagonal Mn_5Si_3-type ($P6_3/mcm$) and orthorhombic Y_5Bi_3-type ($Pnma$) structures exist for the Zr_5Sb_3 compound. The former appears nonstoichiometric as Zr_5Sb_{3+x} with $0 \leqslant x \leqslant 0.4$, while the latter forms stoichiometrically but only stable at high temperature above 1200 °C.[7] To further investigate how the nonstoichiometry affects the superconducting properties, samples with nominal compositions of Zr_5Sb_3 and $Zr_5Sb_{3.3}$ have been made through solid-state sintering process. Different stoichiometric materials were mixed thoroughly and pressed into a pellet inside a glove box. The pellets were initially sealed in a Nb tube under Ar, subsequently sealed in the quartz jacket under vacuum, and then heated up very slowly to 1000 °C for 5 d. The lattice parameter increases for $Zr_5Sb_{3.3}$ [$a = b = 8.577(2)$ Å and $c = 5.874(2)$ Å], as compared to those of Zr_5Sb_3, clearly show the difference of the Sb content and are consistent with previous studies.[7] As illustrated in Fig. 8(a), both the onset T_c and shielding fraction decrease in the $Zr_5Sb_{3.3}$ sample. As previous studies indicated, the extra Sb in Zr_5Sb_{3+x} occupies the octahedral interstitial sites formed by the Zr trigonal antiprism,[7] and our results show that superconductivity in Zr_5Sb_3 is suppressed when the interstitial sites are filled by Sb atoms. We have further tested the influence of Z = O and C, which are introduced to Zr_5Sb_3 through arc-melting and sintering processes. The Zr_5Sb_3O and Zr_5Sb_3C were made through sintering and the arc-melting process according to Ref. 8 by nominal composition. The $Zr_5Sb_3O_x$ was made though the arc-melting process with reduced O_2 atmosphere (2.5% O_2 balanced with argon), although the exact O content is yet to be determined. Only a small diamagnetic signal below 2 K was detected in $Zr_5Sb_3O_x$, and no superconductivity was observed in Zr_5Sb_3O and Zr_5Sb_3C samples [Fig. 8(a)], further proving that superconductivity is not favored by interstitial-filled compounds of Zr_5Sb_3. This is also consistent with previous theoretical calculations that the formation of the Zr-Z bond significantly reduces the Zr1-Zr1 bonding from the trigonal antiprism construction and thus might reduce the DOS at the Fermi surface and suppress the superconducting signal.

Chemical doping with different species has also been carried out. Ti doping by 5% has effectively suppressed the superconducting transition from 2.3 K down to 2 K [Fig. 8(b)], and there is no superconducting signal observed in the 10% Ti-doped sample. This demonstrates that the Ti has been doped into the structure. However, the superconductivity seems pretty robust and stays at ~2.3 K with 5% of either Hf or Y doping [Fig. 8(b)]. Chemical analysis from scanning electron microscope-energy dispersive x-ray (SEM-EDX) clearly shows the homogeneous distribution of Hf, Y, and Ti within the grains of the samples. Therefore, the effects of Y, Hf, and Ti substitution on the superconductivity of Zr_5Sb_3 are rather different.

In summary, we have carried out magnetization, electrical resistivity, and specific heat measurements, and band structure calculations on Zr_5Sb_3 and Zr_5Sn_3. The results show bulk superconductivity with a $T_c \sim 2.3$ K in Zr_5Sb_3, representing the first superconductor discovered in the large family of Mn_5Si_3 structure type. No superconductivity above 2 K was detected in Zr_5Sn_3, attributable to its low DOS at the Fermi level and absence of strongly phonon-coupled bands around the Fermi energy given by the band structure calculations. Detailed doping studies have shown that superconductivity in Zr_5Sb_3 is rather robust with Hf and Y substitution of Zr, but suppressed by Ti substitution; it is also suppressed by interstitial filling in Zr_5Sb_3Z by Z = Sb, C, or O. In view of the large number of compounds in the Mn_5Si_3 structure family, more superconductors, with some of higher T_c, are expected. An extensive search for superconductivity in this and related compound families is underway.

The work in Houston is supported in part by US Air Force Office of Scientific Research (AFOSR) Grant No. FA9550-09-1-0656, the T.L.L. Temple Foundation, the John J. and Rebecca Moores Endowment, and the State of Texas through the Texas Center for Superconductivity at the University of Houston. Z.P.Y. and G.K. are supported by the US Air Force Office of Scientific Research Multidisciplinary University Research Initiative program.

*Authors to whom correspondence should be addressed: blv@uh.edu; cwchu@uh.edu

[1]F. Steglich, J. Aarts, C. D. Bredl, W. Lieke, D. Meschede, W. Franz, and H. Schäfer, Phys. Rev. Lett. **43**, 1892 (1979).
[2]J. G. Bednorz and K. A. Müller, Z. Phys. B **64**, 189 (1986).
[3]M. K. Wu, J. R. Ashburn, C. J. Torng, P. H. Hor, R. L. Meng, L. Gao, Z. J. Huang, Y. Q. Wang, and C. W. Chu, Phys. Rev. Lett. **58**, 908 (1987).
[4]Y. Kamihara, T. Watanabe, M. Hirano, and H. Hosono, J. Am. Chem. Soc. **130**, 3296 (2008).
[5]Data from Inorganic Crystal Structure Database, available at http://icsd.fiz-karlsruhe.de/ Accessed October 10, 2013.
[6]E. Garcia and J. D. Corbett, J. Solid State Chem. **73**, 440 (1988).
[7]E. Garcia and J. D. Corbett, Inorg. Chem. **27**, 2353 (1988).
[8]E. Garcia and J. D. Corbett, Inorg. Chem. **29**, 3274 (1990).
[9]J. D. Corbett, E. Garcia, A. M. Guloy, W. M. Hurng, Y. U. Kwon, and E. A. Leon-Escamilla, Chem. Mater. **10**, 2824 (1998).
[10]Y. U. Kwon and J. D. Corbett, Chem. Mater. **2**, 27 (1990).
[11]H. Padamsee, J. E. Neighbor, and C. A. Shiffman, J. Low. Temp. Phys. **12**, 387 (1973).
[12]N. R. Werthamer, E. Helfand, and P. C. Hohenberg, Phys. Rev. **147**, 295 (1966).
[13]Z. P. Yin, A. Kutepov, and G. Kotliar, Phys. Rev. X **3**, 021011 (2013).
[14]P. Blaha, K. Schwarz, G. K. H. Madsen, D. Kvasnicka, and J. Luitz, *WIEN2K: An Augmented Plane Wave + Local Orbitals Program For Calculating Crystal Properties* (Vienna University of Technology, Vienna, Austria, 2001); J. P. Perdew, K. Burke, and M. Ernzerhof, Phys. Rev. Lett. **77**, 3865 (1996).